



Article

Dynamic Analysis of the Thermo-Deformation Treatment Process of Flat Surfaces of Machine Parts

Volodymyr Gurey ¹, Pavlo Maruschak ^{2,*}, Ihor Hurey ^{1,3}, Volodymyr Dzyura ², Tetyana Hurey ⁴
and Weronika Wojtowicz ⁵

¹ Department of Robotics and Integrated Mechanical Engineering Technologies, Lviv Polytechnic National University, 12, Bandera St., 79013 Lviv, Ukraine; vgurey@gmail.com (V.G.); ihor.hurey@gmail.com (I.H.)

² Department of Wheel Vehicles, Ternopil Ivan Puluj National Technical University, 56, Ruska St., 46001 Ternopil, Ukraine; volodymyrdzyura@gmail.com

³ Faculty of Mechanics and Technology, Rzeszow University of Technology, 12, Powstancow Warszawy St., 35-959 Rzeszow, Poland

⁴ Department of Transport Technologies, Lviv Polytechnic National University, 12, Bandera St., 79013 Lviv, Ukraine; tetiana.a.hurei@lpnu.ua

⁵ Faculty of Mechanical Engineering and Aeronautics, Rzeszow University of Technology, 12, Powstancow Warszawy St., 35-959 Rzeszow, Poland; wwktmiop@prz.edu.pl

* Correspondence: maruschak.tu.edu@gmail.com

Abstract: Thermo-deformation treatment refers to methods of strengthening during which strengthened layers with a nanocrystalline structure are formed in the surface layers by modifying the metal surface layer, which changes its phase and structural and chemical compositions, reduces grain size, and improves performance. Grinding of the metal structure was achieved by combining two methods simultaneously during this treatment: the action of a highly concentrated energy source on the surface layer and intense plastic deformation. The source of highly concentrated energy was generated in the contact zone of the tool-disc, which rotates at high speed during friction on the treated surface. Intense deformation was achieved due to the grooves on the tool's working surface. Dynamic analysis of the thermo-deformation treatment process of flat surfaces of machine parts and a calculation scheme of the surface grinder machine's elastic system, which is the three-mass model, were developed. When the groove width increased from 4 mm to 8 mm, the force amplitude in the contact zone increased from 10 N to 75 N. Accordingly, the thickness of the nanocrystalline layer increased from 190–220 μm to 250–260 μm , and its hardness increased from 9.3 GPa to 11.1 GPa.

Keywords: friction hardening; strengthening; white layer; nanocrystalline structure; mathematical model



Citation: Gurey, V.; Maruschak, P.; Hurey, I.; Dzyura, V.; Hurey, T.; Wojtowicz, W. Dynamic Analysis of the Thermo-Deformation Treatment Process of Flat Surfaces of Machine Parts. *J. Manuf. Mater. Process.* **2023**, *7*, 101. <https://doi.org/10.3390/jmmp7030101>

Academic Editor: Mark J. Jackson

Received: 13 April 2023

Revised: 13 May 2023

Accepted: 18 May 2023

Published: 20 May 2023



Copyright: © 2023 by the authors. Licensee MDPI, Basel, Switzerland. This article is an open access article distributed under the terms and conditions of the Creative Commons Attribution (CC BY) license (<https://creativecommons.org/licenses/by/4.0/>).

1. Introduction

The operational reliability of products is one of the most important parameters of the quality of machine parts and is defined by such indicators as wear resistance, corrosion resistance, fatigue and corrosion-fatigue strength, the strength of fits and mating parts, etc. [1,2]. The accuracy and quality of manufactured surfaces and the condition of the surface layers of parts directly affect the performance of machines. During any type of operation, destruction begins on the surface of the part [3,4]. Increasing the durability of machine parts is achieved by forming the appropriate stereometric parameters of the machined surfaces of the parts and the properties of the metal surface layer [5,6]. The set parameters of the treated surfaces can be obtained using technological methods that belong to a new direction—surface engineering [7,8]. It allows for the carrying out of surface strengthening of machine parts by a method of modification of the metal's surface layer [9,10]. The surface layer of the metal is strengthened by changing its structure and chemical and phase composition, reducing the grain size to the nanoscale, etc., during modification. It should be noted that the crystal lattice remains the same, as only its dimensions change [11,12].

Modification of the surface layers of metal in machine parts can be carried out by technological methods using highly concentrated energy sources, namely laser [13], plasma [14], electron beam [15,16], frictional strengthening [17,18], and other treatments [19–21]. In these methods of processing under the influence of concentrated energy flows, small volumes of the surface layer of the metal are heated at a high rate to temperatures above the point of phase transformations [22,23]. After removing the heat source, the surface layers of the metal are cooled at a high rate by transferring the heat to the depth of the part [24,25]. Strengthened nanocrystal layers with specific physical, mechanical, and operational properties are formed in the surface layers of the metal.

Forming, changing the structure, and reducing the grain size of the strengthened surface layer of metal are also obtained by methods of intense plastic deformation [26,27]. The surface layer formed during rapid heating and cooling, as well as after intense plastic deformation, has changed physical and mechanical characteristics, different phase states and chemical compositions of the metal, the presence of residual compressive stresses, and formed specific structures [28]. Technological methods that modify the surface layer of metal reduce the grain size when it is in at least one direction that is less than 100 nm (the process of forming the nanostructure), which is significantly smaller than the base material. Surface layers with nanocrystalline structures have unique physical, mechanical, and chemical properties that improve the performance of parts [9,11,27,29,30].

The developed method of thermo-deformation treatment (strengthening) of machine parts—which belongs to the methods of surface strengthening that use high-intensity heat sources—using a tool with transverse grooves on the working surface allows for the combination of two parallel methods of strengthening—strengthening that uses a high-intensity heat source and intensive plastic deformation [9,11,30]. The friction of the working surface of the tool at high speed on the processed surface forms a highly concentrated source of energy, and transverse grooves on its periphery provide high-intensity shock loads.

Thermo-deformation treatment refers to the methods of forming hardened surface layers with a nanocrystalline structure on massive parts. During this treatment, the action of a highly concentrated heat energy flow and intense plastic deformation are simultaneously combined, the source of which is the high-speed friction of a metal tool-disc on the treated surface in the zone of mutual contact. The intensity of deformation of the metal surface layer is increased by increasing the width of the grooves on the tool's working surface.

The method of thermo-deformation treatment belongs to finishing operations. During finishing operations, it is attempted to reduce the dynamic components of the processing procedure. In this case, the dynamic components of the process are increased to intensify the process of hardening (strengthening) and to improve the conditions for the formation of hardened (strengthened) layers. The aim of this work was the dynamic analysis of the thermo-deformation treatment process of flat surfaces of machine parts to determine the magnitude of impact loads in the zone of contact of the tool with the treated flat surface. Thermo-deformation treatment is one of the surface strengthening methods that uses highly concentrated energy flows. Highly concentrated energy flow is formed during high-speed (60–90 m/s) friction of a tool on the treated part (sample) in the zone of contact. The heating rate of the contact zone reaches $4 \cdot 10^5$ – $5 \cdot 10^6$ K/s. The surface layers of the metal are heated to temperatures above the point of phase transformations (A_{c3}). After removing the heat source, the heated surface layer is cooled at a high rate ($6 \cdot 10^4$ – $9 \cdot 10^5$ K/s) by transferring heat to the depth of the metal part. There is simultaneous high-speed shear deformation of the treated surface in the contact zone. Nanocrystalline structures (white layer) are formed in the surface layer of parts due to high-speed heating and cooling and intensive shear deformation.

2. Materials and Methods

Thermo-deformation strengthening of the flat surfaces of machine parts in terms of the performance and kinematics of the process is similar to technological grinding methods (Figure 1a). For their performance, surface grinding machines are used with the

modernization of the rotation drive unit to ensure a linear speed of 60–90 m/s at the tool periphery. A metal tool-disc is mounted instead of an abrasive wheel. The overall and mounting dimensions of the metal tool-disc correspond to the dimensions of the abrasive wheel that is used on this grinding machine.

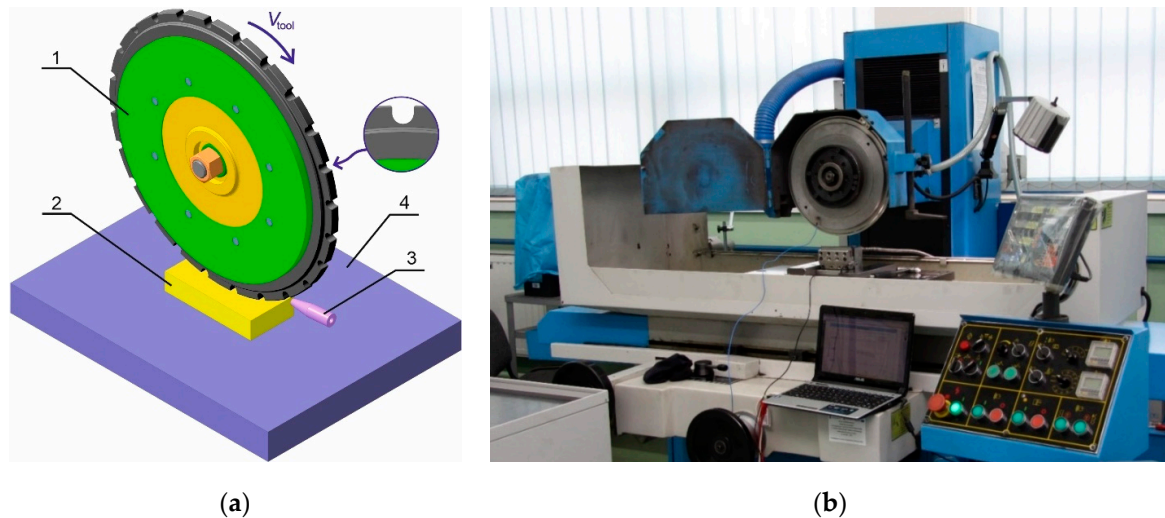


Figure 1. Scheme of thermo-deformation treatment of flat surfaces of machine parts (a): 1—tool, 2—treated flat surface of a part, 3—nozzle for provision of the technological medium, 4—machine table, V_{tool} —linear speed; (b) HFS 3063 VS surface grinder from Knuth (Wasbek, Germany).

An upgraded HFS 3063 VS surface grinder from Knuth (Wasbek, Germany) was used to perform thermo-deformation strengthening of flat surfaces (Figure 1b). The machine's spindle drive was replaced with a different one with a higher frequency and the ability to control speed using a DC motor and a control panel from Siemens (Munich, Germany). The bearings of the spindle assembly were calculated for operation at higher speeds and with higher loads. The tool was made of stainless steel. The external diameter D_{tool} of the tool-disc was 360 mm, and the width of the tool's working part b_{tool} was 6–8 mm (Figure 2). The tool was set up into a mandrel holder that was included in the kit with the surface grinder machine. We performed static balancing before mounting the tool-disc assembly with the mandrel holder on the surface grinder machine [9,30].

To improve the processes of formation, a strengthened layer with a nanocrystal structure, namely increasing its thickness and microhardness and reducing the grain size of the structure, a tool with transverse grooves on its periphery was used during thermo-deformation strengthening. There is a patent in Ukraine (No. 123883) [31] and a patent in Poland (No. 240972) [32] for the design of this tool. When using a tool with transverse grooves on its periphery, a discontinuous, highly concentrated energy flow (heating and cooling cycles) is formed, and a source of high-frequency deformation is formed in the zone of contact of the tool with the treated surface. During thermo-deformation strengthening with the tool with transverse grooves on its periphery, in the surface layers of the metal of the treated surfaces of the parts, two processes take place simultaneously: the action of a highly concentrated energy source and intensive shear deformation.

On the working part, the tool has transverse grooves with the same circular pitch, alternating smooth parts, and a groove with the same frequency. The minimum value of the groove width was selected based on the condition that the tool's working surface was guaranteed to completely lose contact with the sample. The tool is pressed to the sample's treated surface during thermo-deformation strengthening with a force of 500–1200 N, and the effect of this force in the contact zone forms a radial component of the force between the tool and the sample. In addition, there is a tangential component of the force between the tool and the sample that occurs by rotation of the tool in the contact zone, which determines the value of the heat flow. When the groove is over the contact zone between the tool and

the part at this time point, the contact zone is unloaded, and the normal and tangential components of the force of the tool on the part equal zero. The influence of the heat source is suspended. A sharp (impact) load is applied to the contact zone, followed by high-speed friction of the smooth part of the tool on the samples' surfaces when the tool's next working smooth surface comes into contact. The action of the source of intensive thermal energy is reset in the contact zone. Thermal energy, shear deformation, and impact loads are impulsively applied to the contact zone. The frequency of impact loads is determined by the number of grooves on the working part of the tool. These processes form strengthened layers with a nanocrystalline structure, which have greater thickness, increased hardness, and more fine-grained structure compared to treatment with a tool that has a smooth working surface [11].

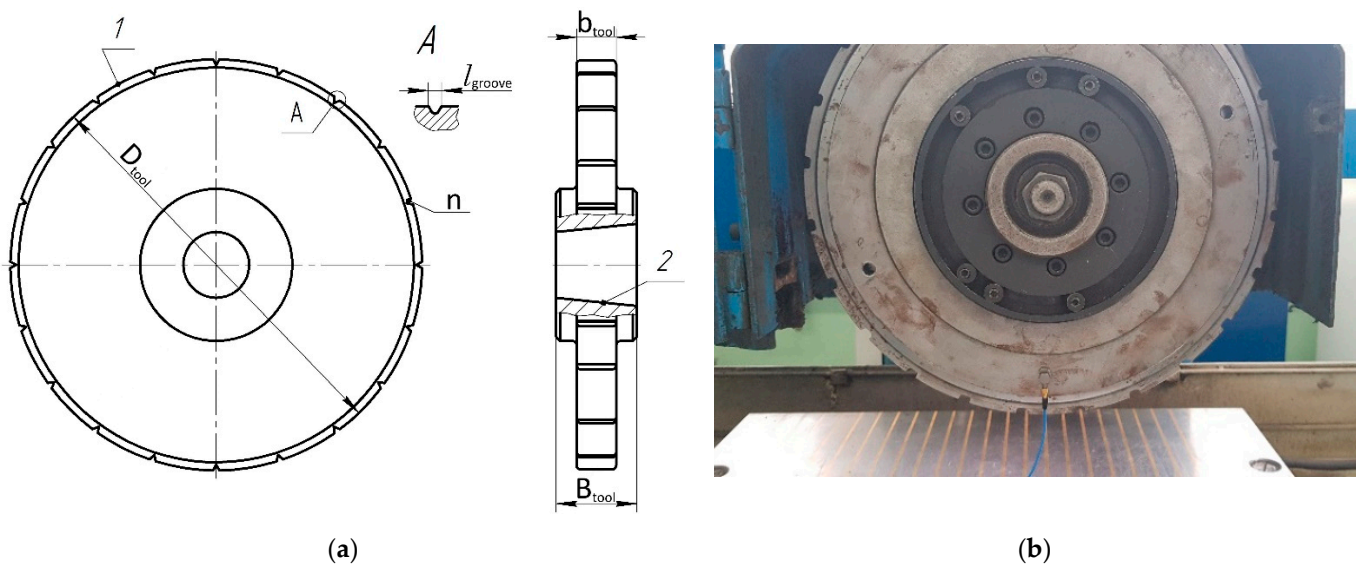


Figure 2. The tool with transverse grooves on its periphery: sketch (a) and tool mounted on surface grinder (b): 1—working smooth surface of the tool, 2—Morse taper, D_{tool} —external diameter, B_{tool} —width of the tool, b_{tool} —width of the working part of the tool, l_{groove} —width of the groove, n —number of grooves.

Thermo-deformation strengthening of flat surfaces according to the kinematics of the process is similar to the grinding of flat surfaces (Figure 3), so the friction force in the contact area between the tool and the part can be divided into three components: normal component, which acts on the radius of the tool, perpendicular to the axis of its rotation; tangential component, which acts tangentially to the working surface of the tool parallel to the workpiece surface; and transverse component, which acts parallel to the axis of rotation of the tool in the direction opposite to the feed movement. Measurements of the components of friction forces in the contact area between the tool and the part were performed using a three-component type 9121 dynamometer from Kistler (Winterthur, Switzerland) (Figure 4). Experimental samples were made of steel 41Cr4 (quench-hardening and low-temperature tempering) with a size of 15mm × 30mm × 100 mm. The chemical composition of the steel is as follows: mass %: 0.40 C; 0.78 Mn; 0.26 Si; 1.12 Cr; 0.01 S; 0.01 P; Fe: balance. A three-component dynamometer with a fixed sample was mounted on the magnetic plate of the surface grinder machine.

The Type 9121 Kistler three-component dynamometer uses a piezoelectric force component measurement system. Due to its high natural frequencies, it can measure high-speed processes. The piezoelectric dynamometer is connected to a multi-channel high-quality amplifier-converter (National Instruments, Austin, TX, USA), which has an interface for connection to a computer. LabView software was used to process the results of the force component studies.

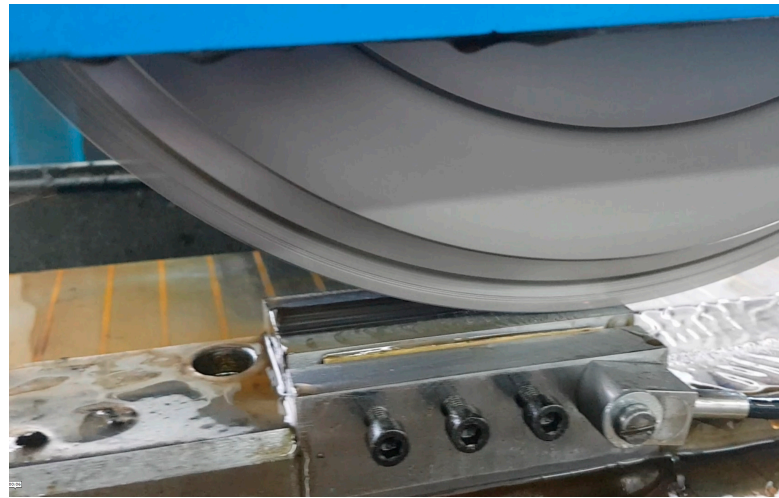


Figure 3. View of the sample's surface during processing (the black surface is the already-processed surface).

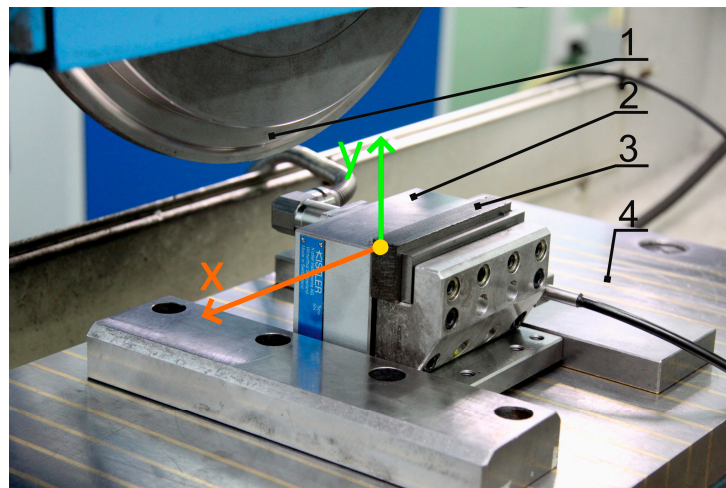


Figure 4. Three-component dynamometer type 9121 (Kistler, Switzerland): 1—tool, 2—dynamometer, 3—sample, 4—machine table.

Experimental studies were conducted to determine the normal and tangential components of the friction force in the contact zone between the tool and the treated surface during thermo-deformation strengthening of the samples' flat surfaces made of steel 41Cr4 (quench-hardening and low-temperature tempering). A metal tool-disc made of stainless steel X10CrNiTi18–10 (EU) was installed on a modernized machine (HFS 3063 VS by KNUTH). The tool's outer diameter was 360 mm, the width of the working surface was 6 mm, and 24 grooves were formed on the working surface of the tool. The linear speed on the tool's peripheral working part was 70 m/s, and the speed of movement of the grinder machine table was 4 m/min.

Mathematical Model

Notation and units: ω —angular velocity of the tool's rotation, s^{-1} ; x_1, y_1 —displacements of the spindle headstock in the horizontal and vertical planes, m; x_2, y_2 —displacements of the tool in the horizontal and vertical planes, m; x_3, y_3 —displacements of the machine table in the horizontal and vertical planes; D_{tool} —external diameter of the tool, m; n —the number of grooves or working smooth surfaces of the tool; F_{rc} —the force of friction between the treated surface of the tool's working smooth surface and the sample, N; m_1 —the spindle head's mass, kg; m_2 —the tool's mass, kg; m_3 —the parts' (workpiece's) mass, kg; c_1 and c_2 —stiffness

between the column guideways and the machine headstock in the horizontal and vertical planes, N/m; c_3 and c_4 —stiffness of the machine spindle supports in the horizontal and vertical planes, N/m; c_5 and c_6 —stiffness of the machine table in the horizontal and vertical planes, N/m; c_7 —contact stiffness between the part and the tool, N/m; μ_1 and μ_2 —damping coefficient between the column guideways and the machine headstock in the horizontal and vertical planes, Ns/m; μ_3 and μ_4 —damping coefficient of the machine spindle supports in the horizontal and vertical planes, Ns/m; μ_5 and μ_6 —damping coefficient of the machine table in the horizontal and vertical planes, Ns/m; μ_7 —damping coefficient between the tool and sample (internal damping), Ns/m.

The first stage of dynamic analysis of the thermo-deformation treatment process of the flat surfaces of machine parts is to develop a calculation scheme of the machine’s elastic system and describe it as a three-mass model. To do this, the surface grinder machine was divided into a number of units, each one of which represents a separate mass (Figure 5). It is very important to define the part or unit that will be selected as a part with a conditionally infinite mass relative to which the movements of the other masses are determined. The bed of the surface grinder machine to which all the other masses (the weight of the spindle head, the weight of the tool, and the weight of the machine table with the part) are “attached” was accepted as a part with conditionally unlimited mass. Elastic and damping bonds describe the relationship between individual masses.

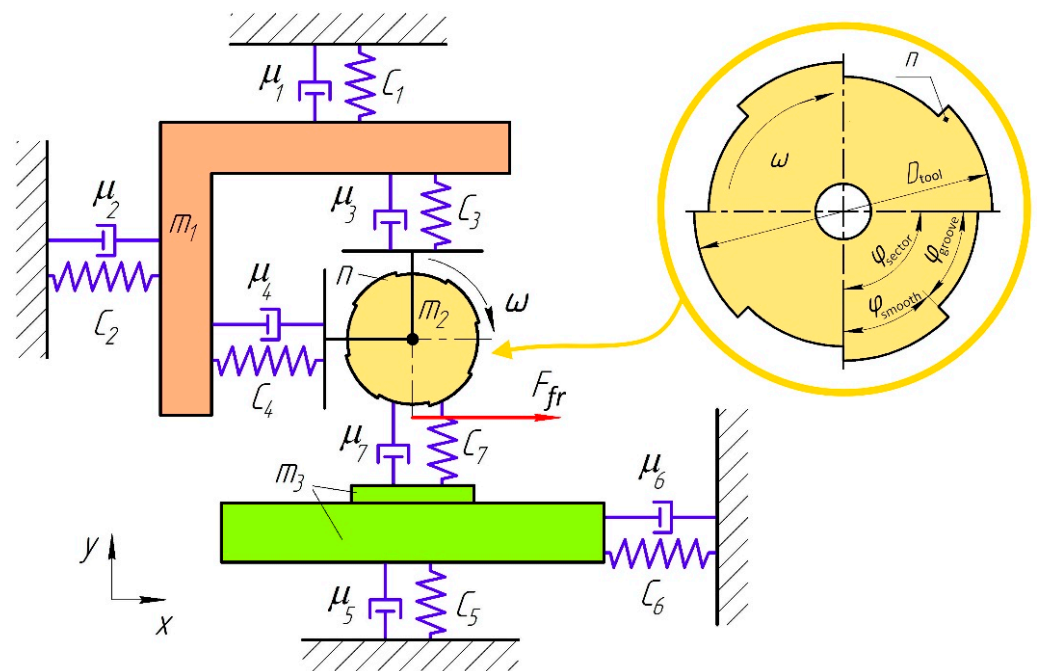


Figure 5. Calculation scheme of the grinder machine.

The pressing force of the tool to the sample was proposed to be defined in an implicit form, i.e., to set through the relative movement (Δy) of the spindle head in the direction of the surface grinder machine’s table in this mathematical model. Having set a certain amount of displacement Δy , the pressing force is generated by the composition of the stiffness of all the elements in the machine’s oscillatory circuit. Most machines cannot measure the components of the forces that occur during the treatment process. Nevertheless, they all have a limb or optical ruler that can be used to determine tool movement, which served as this choice’s main idea. The normal component of the force that occurs during processing has been pre-determined by experimental studies [29].

The generalized coordinates $q_{i,j}$ (where the number of masses is $i = 1, 2, 3$ and the number of coordinates is $j = 1, 2$) in our case will be:

- for the spindle head with the mass m_1 : $q_{11} = x_1$; $q_{12} = y_1$.

- for the tools with the mass m_2 : $q_{21} = x_2$; $q_{22} = y_2$.
- for the parts (workpiece) with the mass m_3 : $q_{31} = x_3$; $q_{32} = y_3$.

The motion of the system can be described by differential equations built based on Euler–Lagrange equations [33–36]:

$$\frac{d}{dt} \left(\frac{\partial T}{\partial \dot{q}_{i,j}} \right) - \frac{\partial T}{\partial q_{i,j}} + \frac{\partial V}{\partial q_{i,j}} + \frac{\partial D}{\partial \dot{q}_{i,j}} = Q_{q_i}, \tag{1}$$

where T is the kinetic energy of the system; V is the potential energy of the system; D is the energy dissipation function in the system (Rayleigh dissipation function); and $Q_{q_{i,j}}$ are the generalized forces that refer to the corresponding generalized coordinates x_i and y_i .

We should accept the following assumptions when forming a mathematical model: we assume that the law of change of rigidity in the elastic elements of the system does not go beyond linearity, and it corresponds to Hooke’s law. This is justified, provided that there are small deviations of the spring from the equilibrium position; we will consider the mechanical system of the machine as one consisting of absolutely rigid bodies connected by ideal holonomic ties and elastic elements of strictly defined rigidity. Into the dynamic model, we will introduce coefficients of viscous friction that are proportional to the speed of movement of the moving sliders along the corresponding guide axes and that reflect the energy dissipation in the corresponding elastic elements of the system in the form of dampers [33,34,36,37].

Thus, using the ratio of the forces’ virtual work $\sum \delta A(F_k)$ that acts on each element to the increment of a certain generalized coordinate $\delta q_{i,j}$ for the corresponding masses, the generalized force can be determined from the next equation:

$$Q_{i,j} = \frac{\delta A_{i,j}}{\delta q_{i,j}}. \tag{2}$$

Therefore, for the spindle head, the generalized force will look as follows:

$$\begin{aligned} Q_{x_1} &= 0, \\ Q_{y_1} &= \frac{N \cdot \delta y_1}{\delta y_1} = N. \end{aligned} \tag{3}$$

For the tool:

$$\begin{aligned} Q_{x_2} &= f \frac{(N - N_{23}) \cdot \delta x_2}{\delta x_2} = f(N - N_{23}), \\ Q_{y_2} &= \frac{N_{23} \cdot \delta y_2}{\delta y_2} = N_{23}. \end{aligned} \tag{4}$$

For the part:

$$Q_{x_3} = f \frac{(N - N_{23}) \cdot \delta x_3}{\delta x_3} = f(N - N_{23}); \quad Q_{y_3} = \frac{N_{23} \cdot \delta y_3}{\delta y_3} = N_{23}. \tag{5}$$

where f is the friction coefficient between the tool and the sample and N is the tool’s force of the normal pressure to the sample, which is formed due to the displacement y_0 of the spindle head in the direction of the sample (depth of cut during the technological operation of grinding), i.e.:

$$N = c_y^* \cdot y_0, \tag{6}$$

where y_0 is the displacement of the spindle head in the direction of the sample when the tool’s working smooth surface is in contact with the treated surface of the part, i.e., by means of this displacement, the mutual pressing force is formed; c_y^* is the reduced stiffness of the system in the vertical plane:

$$\frac{1}{c_y^*} = \frac{1}{c_1 + c_3} + \frac{1}{c_5 + c_7}. \tag{7}$$

The formation of the pressing force, as described above, happens by moving the spindle head (lowering) in the direction of the part through the transmission from the screw and the nut to the value y_0 . It is assumed to be constant during processing (i.e., displacement, which is controlled by the machine limb and forms the pressing force between the tool's working smooth surface and the treated surface of the part) [9,11,30]. Due to the geometry of the tool (alternating the tool's working smooth surface with the groove), there is a decrease in the pressing force between the tool and the part by the amount of displacement y_{23} .

$$y_{23} = \begin{cases} 0, & \text{when } \omega t = (0 \dots \varphi_{smooth}) + \frac{2\pi}{n} \cdot m \\ (R - R \cdot \cos \omega t), & \text{when } \omega t = \left(\varphi_{smooth} \dots \frac{\varphi_{groove}}{2} \right) + \frac{2\pi}{n} \cdot m \\ (R - R \cdot \cos \omega t) - \left(R - R \cdot \cos \left(\frac{\varphi_{sector} - \varphi_{smooth}}{2} \right) \right), & \text{when } \omega t = \left(\frac{\varphi_{groove}}{2} \dots \varphi_{smooth} \right) + \frac{2\pi}{n} \cdot m \end{cases} \quad (8)$$

$m = 0, 1, 2 \dots (n - 1)$

where R is the diameter of the tool $R = D_{tool}/2$ and n is the number of smooth parts of the tool.

The normal force changes in accordance with the condition of contact of the tool's periphery with the sample's treated surface, i.e., the contact of the tool's working smooth part with the sample's treated surface, as well as the position of the tool's groove above the sample's treated surface, form the analytical dependences of the generalized forces Q_i , as follows:

$$\begin{aligned} Q_{y_1} &= N; & Q_{y_2} &= N_{23}; \\ Q_{x_1} &= 0; & Q_{x_2} &= F_{fr} = f \cdot (N - N_{23}); \\ |Q_{y_2}| &= |-Q_{y_3}|; & |Q_{x_2}| &= |-Q_{x_3}|. \end{aligned} \quad (9)$$

where N_{23} is the force that reduces the force of the normal pressure of the tool to the part, which is formed due to the displacement y_{23} , caused by alternating changes of the smooth part and the groove during rotation of the tool:

$$N_{23} = c_y^* \cdot y_{23}, \quad (10)$$

Additionally, it is necessary to describe the case when the groove on the periphery of the tool is narrow and allows for the stopping of the heat flow but does not allow the tool to freely get out of contact with the part (Figure 6). Therefore, the minimum value of the pressing force is determined by the dependence:

$$\begin{aligned} & \text{If } y_0 < \Delta R, \\ & \text{then } |N_{min}| = c_y^* \cdot (y_0 - \Delta R) \text{ when } \omega t = \left(\varphi_{smooth} \dots \varphi_{sector} \right) + \frac{2\pi}{n} \cdot m \\ & \Delta R = R - R' = R - R \cdot \cos \left(\frac{\varphi_{sector} - \varphi_{groove}}{2} \right). \end{aligned} \quad (11)$$

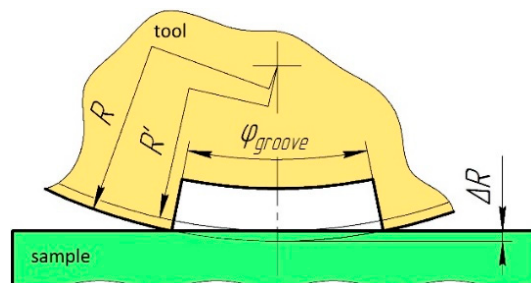


Figure 6. Contact of the tool in the contact area (groove above the sample's treated surface): R —radius of the tool, R' —value from the center of the tool normal to the processing sample when the groove is symmetrical on the processing zone, ΔR —difference between R and R' , and φ_{groove} —size of the groove.

To start writing the left part of the Euler–Lagrange equations, we need to find the derivatives of the expression of kinetic energy T :

For the spindle head:

$$\begin{aligned} \frac{\partial T}{\partial \dot{q}_{11}} &= \frac{\partial T}{\partial \dot{x}_1} = m_1 \dot{x}_1; & \frac{\partial T}{\partial \dot{q}_{12}} &= \frac{\partial T}{\partial \dot{y}_1} = m_1 \dot{y}_1; \\ \frac{d}{dt} \left(\frac{\partial T}{\partial \dot{x}_1} \right) &= m_1 \ddot{x}_1; & \frac{d}{dt} \left(\frac{\partial T}{\partial \dot{y}_1} \right) &= m_1 \ddot{y}_1. \end{aligned} \tag{12}$$

For the tool:

$$\begin{aligned} \frac{\partial T}{\partial \dot{q}_{21}} &= \frac{\partial T}{\partial \dot{x}_2} = m_2 \dot{x}_2; & \frac{\partial T}{\partial \dot{q}_{22}} &= \frac{\partial T}{\partial \dot{y}_2} = m_2 \dot{y}_2; \\ \frac{d}{dt} \left(\frac{\partial T}{\partial \dot{x}_2} \right) &= m_2 \ddot{x}_2; & \frac{d}{dt} \left(\frac{\partial T}{\partial \dot{y}_2} \right) &= m_2 \ddot{y}_2. \end{aligned} \tag{13}$$

For the part:

$$\begin{aligned} \frac{\partial T}{\partial \dot{q}_{31}} &= \frac{\partial T}{\partial \dot{x}_3} = m_3 \dot{x}_3; & \frac{\partial T}{\partial \dot{q}_{32}} &= \frac{\partial T}{\partial \dot{y}_3} = m_3 \dot{y}_3; \\ \frac{d}{dt} \left(\frac{\partial T}{\partial \dot{x}_3} \right) &= m_3 \ddot{x}_3; & \frac{d}{dt} \left(\frac{\partial T}{\partial \dot{y}_3} \right) &= m_3 \ddot{y}_3. \end{aligned} \tag{14}$$

And

$$\frac{\partial T}{\partial x_i} = 0; \quad \frac{\partial T}{\partial y_i} = 0. \tag{15}$$

The elastic elements accumulate the potential energy V in the system, and the following dependence is used to find it:

$$V = \frac{c_1 \cdot y_1^2}{2} + \frac{c_3 (y_1 - y_2)^2}{2} + \frac{c_7 (y_2 - y_3)^2}{2} + \frac{c_5 \cdot y_3^2}{2} + \frac{c_2 \cdot x_1^2}{2} + \frac{c_4 (x_1 - x_2)^2}{2} + \frac{c_6 \cdot x_3^2}{2}. \tag{16}$$

The next elements on the left part of the Euler–Lagrange equations are the derivatives of the expression of potential energy:

For the spindle head:

$$\frac{\partial V}{\partial x_1} = c_2 x_1 + c_4 x_1 - c_4 x_2; \quad \frac{\partial V}{\partial y_1} = c_1 y_1 + c_3 y_1 - c_3 y_2. \tag{17}$$

For the tool:

$$\frac{\partial V}{\partial x_2} = -c_4 x_1 + c_4 x_2; \quad \frac{\partial V}{\partial y_2} = -c_3 y_1 + c_3 y_2 + c_7 y_2 - c_7 y_3. \tag{18}$$

For the part:

$$\frac{\partial V}{\partial x_3} = c_6 x_3; \quad \frac{\partial V}{\partial y_3} = -c_7 y_2 + c_7 y_3 + c_5 y_3. \tag{19}$$

We assume that the energy dissipation is directly proportional to the velocity, so the dissipative function D for the system is calculated using the following expression:

$$D = \frac{\mu_1 \cdot \dot{y}_1^2}{2} + \frac{\mu_3 (\dot{y}_1 - \dot{y}_2)^2}{2} + \frac{\mu_7 (\dot{y}_2 - \dot{y}_3)^2}{2} + \frac{\mu_5 \cdot \dot{y}_3^2}{2} + \frac{\mu_2 \cdot \dot{x}_1^2}{2} + \frac{\mu_4 (\dot{x}_1 - \dot{x}_2)^2}{2} + \frac{\mu_6 \cdot \dot{x}_3^2}{2}. \tag{20}$$

The last elements on the left part of the Euler–Lagrange equations are the derivatives of the expression of the dissipative function:

For the spindle head:

$$\frac{\partial D}{\partial \dot{x}_1} = \mu_2 \dot{x}_1 + \mu_4 \dot{x}_1 - \mu_4 \dot{x}_2; \quad \frac{\partial D}{\partial \dot{y}_1} = \mu_1 \dot{y}_1 + \mu_3 \dot{y}_1 - \mu_3 \dot{y}_2. \tag{21}$$

For the tool:

$$\frac{\partial D}{\partial \dot{x}_2} = -\mu_4 \dot{x}_1 + \mu_4 \dot{x}_2; \quad \frac{\partial D}{\partial \dot{y}_2} = -\mu_3 \dot{y}_1 + \mu_3 \dot{y}_2 + \mu_7 \dot{y}_2 - \mu_7 \dot{y}_3. \tag{22}$$

For the part:

$$\frac{\partial D}{\partial y_3} = -\mu_7\dot{y}_2 + \mu_7\dot{y}_3 + \mu_5\dot{y}_3; \quad \frac{\partial D}{\partial x_3} = \mu_6\dot{x}_3. \tag{23}$$

Now, the dynamics of a surface grinder machine’s mechanical system can be described by the following mathematical model:

$$\left\{ \begin{array}{l} m_1\ddot{x}_1 + c_2x_1 + c_4x_1 - c_4x_2 + \mu_2\dot{x}_1 + \mu_4\dot{x}_1 - \mu_4\dot{x}_2 = Q_{x_1} \\ m_2\ddot{x}_2 - c_4x_1 + c_4x_2 - \mu_4\dot{x}_1 + \mu_4\dot{x}_2 = Q_{x_2} \\ m_3\ddot{x}_3 + c_6x_3 + \mu_6\dot{x}_3 = -Q_{x_3} \\ m_1\ddot{y}_1 + c_1y_1 + c_3y_1 - c_3y_2 + \mu_1\dot{y}_1 + \mu_3\dot{y}_1 - \mu_3\dot{y}_2 = Q_{y_1} \\ m_2\ddot{y}_2 - c_3y_1 + c_3y_2 + c_7y_2 - c_7y_3 - \mu_3\dot{y}_1 + \mu_3\dot{y}_2 + \mu_7\dot{y}_2 - \mu_7\dot{y}_3 = Q_{y_2} \\ m_3\ddot{y}_3 - c_7y_2 + c_7y_3 + c_5y_3 - \mu_7\dot{y}_2 + \mu_7\dot{y}_3 + \mu_5\dot{y}_3 = -Q_{y_3} \end{array} \right. \tag{24}$$

We assume that at the initial moment of the simulation, the tool is in contact with the sample with a smooth working part; then, the pressure at the initial moment of the simulation will be equal:

$$F_0 = y_0 \cdot c_y^*. \tag{25}$$

Initial conditions:

$$\begin{array}{l} \dot{x}_i|_{t=0} = 0, \quad \dot{y}_i|_{t=0} = 0, \\ x_1|_{t=0} = 0, \quad x_2|_{t=0} = 0, \quad x_3|_{t=0} = 0. \\ y_1|_{t=0} = \frac{F_0}{c_1+c_3}, \quad y_2|_{t=0} = \frac{F_0}{c_1+c_3+c_7}, \quad y_3|_{t=0} = \frac{F_0}{c_1+c_3+c_5+c_7}. \end{array} \tag{26}$$

Modeling of the interaction of the tool’s working smooth part with the sample is carried out using the contact stiffness and damping of the energy of local elastic–plastic deformation. For this reason, it is necessary to introduce an additional condition of checking the mutual contact between the tool’s working smooth part and the sample’s treated surface. In other words, if the tool moves in the opposite direction to the sample, contact stiffness and damping will be lost:

$$\text{If } y_3 - y_2 < 0, \text{ then } c_7 = 0, \mu_7 = 0. \tag{27}$$

3. Results

We started the simulation from no-load running (I-stage); next was the gradual contact of the tool’s working smooth surface with the sample’s treated surface (from the starting point of the tool’s working smooth surface) in two segments (II-stage) (by segments, we mean the tool’s working smooth part and the one groove); and then, the full value of the force of the tool pressure to the part was formed (III-stage). The rotation of the tool happens clockwise with an angular velocity (the speed of the movement of the table with the sample is significantly lower, and in the simulation, we neglected it; the linear speed of rotation of the tool was 60–70 m/s, and the speed of the table of the grinder machine was 2–4 m/min).

Modeling of the dynamic processes of the technological operation of thermo-deformation strengthening of flat surfaces was performed using MATLAB-Simulink software, and the differential equations were solved using the Runge–Kutta method. The process simulation was performed using a tool with transverse grooves, which with the same circular pitch alternated with the smooth surface in turn.

The process of the technological operation of thermo-deformation strengthening of flat parts is similar to the technological operation of flat grinding by kinematics and is performed on a surface grinder. The tool alternately comes into contact with the processed part; after passing the strengthening surface, it comes out of contact with it. Therefore, in the simulation of the load on the part in this model when the tool comes into contact, the pressure should be given by a variable that increases from zero to the operating value. That is, for ease of testing the process, we set the following procedure for forming the pressure of the tool to the part: the first stage was no-load running (idling); with a lack of pressure

when rotating the first segment, the tool was outside the workpiece (tool’s smooth surface and groove, i.e., $\pi/4$); the second stage was a linear increase in the pressure to its specified value during the rotation of the next three segments, the contact of the tool with the part (from $\pi/4$ to 2π); in the third stage, the working pressure, i.e., all the other rotations of the tool, was taken as that which set a constant pressure equal to $F = 500$ N (Figure 7). Additionally, the initial conditions for the movement of all masses in the vertical direction will be zero, i.e., the right-hand side of Equation (24) will be zero.

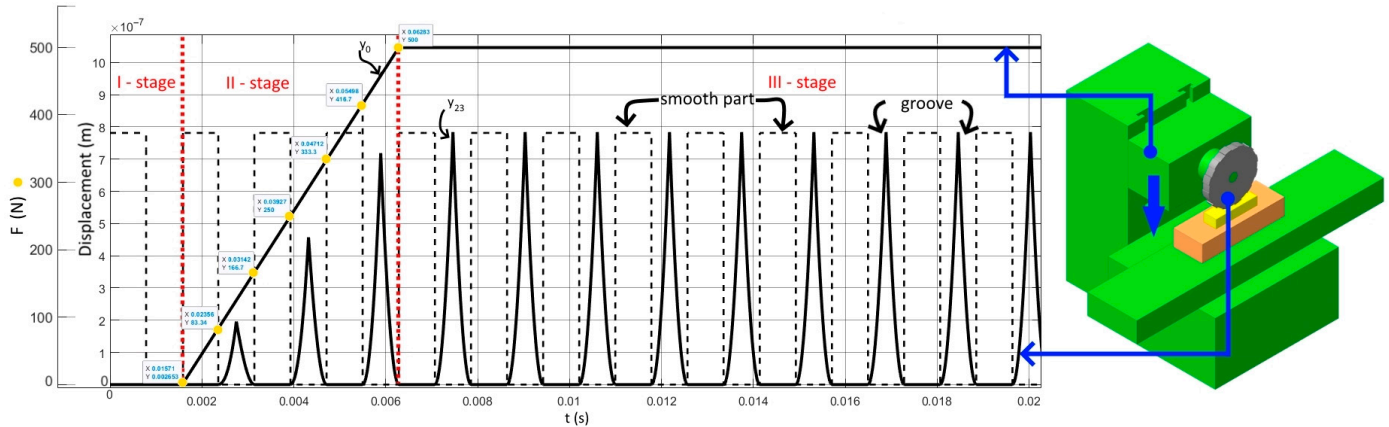


Figure 7. Simulation of pressure by moving the spindle head of the surface grinder machine and the geometry of the tool (The dashed line only shows the location of the smooth parts of the tool (the y-axis has a representative scale)).

Numerical solutions of displacements were made for the following parameters: number of grooves $n = 16$, groove width $l_{groove} = 4$ mm; the force of the pressure of the tool to the sample $F = 500$ N; the tool’s external diameter $D = 260$ mm; and the angular spindle speed $\omega = 500$ s⁻¹. The displacements in the vertical direction y_1, y_2, y_3 of the corresponding mass will be stable and of the same frequency after the value y_0 is equal to the working displacement (Figure 8), i.e., the full working value of the pressure will be formed (full contact of the tool with the processed surface of the part); the velocity of displacement of the tool in the vertical direction is shown in Figure 9.

Displacement of the tool in the horizontal direction (Figure 10a) was caused by friction force, which depends on the pressure of the tool to the part and is variable during the strengthening process. The velocity of displacement of the tool in the horizontal direction is shown in Figure 10b. An important parameter in the study is the reaction that occurs in the contact zone during the processing, which is presented in Figure 11. Modeling of the process of thermo-deformation strengthening of flat parts was performed at several groove widths and pressures (Figures 12 and 13).

It is known that the formation of nanocrystalline structures in the surface layers is particularly influenced by high-frequency deformations of low-amplitude values. When analyzing the obtained numerical solution of system displacements using different values of pressure and groove width, it can be argued that the value of the groove width has a significant effect on the reaction amplitude taking place in the processing area between the tool and the workpiece. For example, when using a tool with a groove in which the groove width is 4 mm, the pressure is 750 N, and the number of grooves on the periphery of the tool is equal to 8 pcs, the reaction amplitude is equal to 10 N. With a groove width of 8 mm, the difference between the maximum and minimum values of the reaction amplitude is 7.5 times higher and is 75 N (Figure 14). However, as the number of grooves on the periphery of the tool increases, the difference between the maximum and minimum values of the amplitude of the reaction decreases. For example, with the same pressure of the tool to the part with the number of grooves equal to 24 pcs and a groove width of 4 mm, the amplitude difference will be equal to 5 N, and with a groove width of 8 mm, the amplitude difference will be 38 N. It should also be noted that the value of the difference between the

maximum and minimum values of the amplitude of the reaction is the same when using the same width of tool at different pressures. That is, if the amount of displacement of the tool to the part that forms the clamping force is greater than the value ΔR (see Figure 6), the difference between the maximum and minimum values of the reaction amplitude will be the same at different clamping forces, but the groove width will be the same.

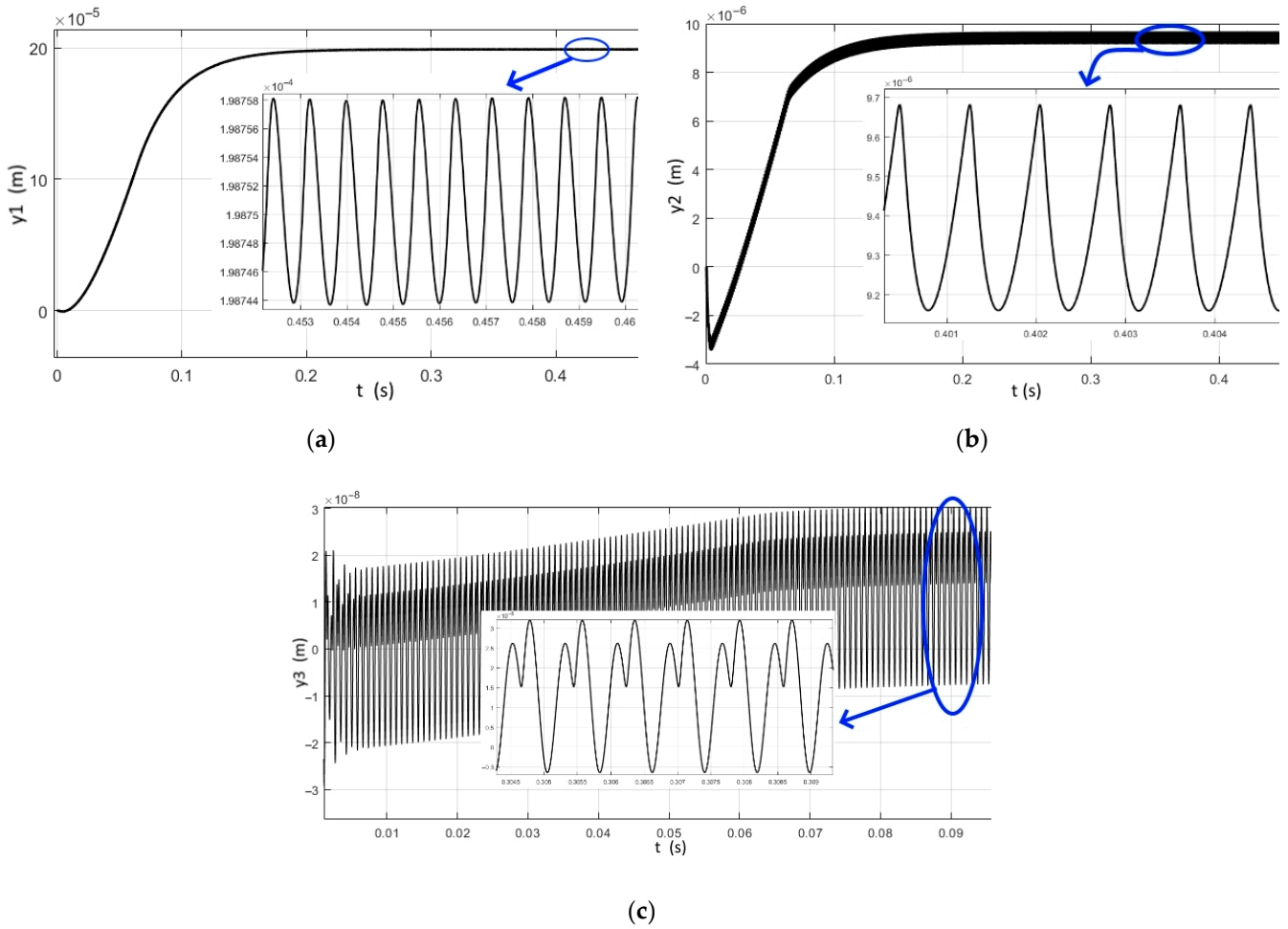


Figure 8. Displacement in the vertical plane: (a) spindle headstock; (b) spindle with tool; (c) table with part.

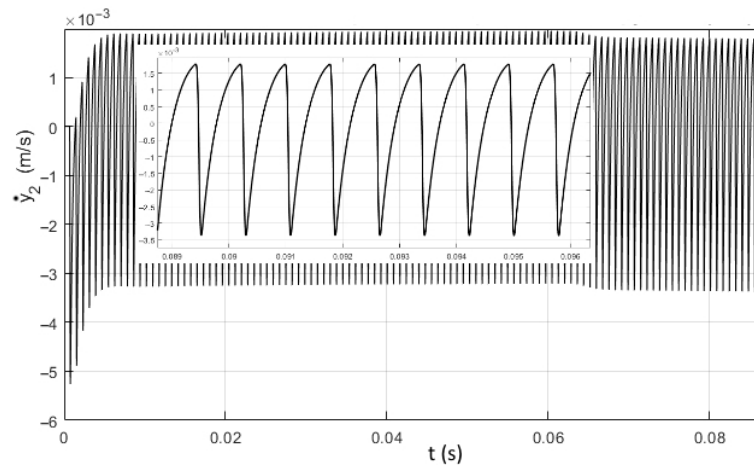


Figure 9. Velocity of displacement of the tool in the vertical plane.

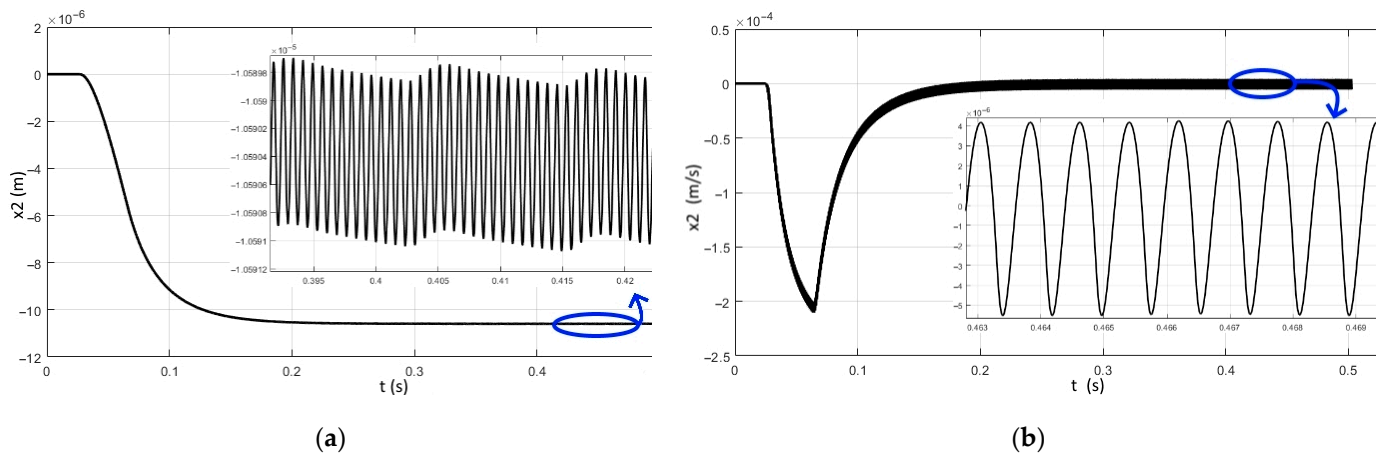


Figure 10. Displacement (a) and velocity (b) of the tool in the horizontal plane.

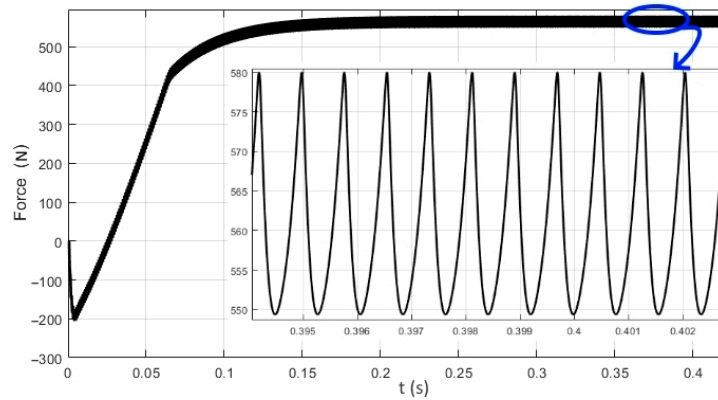


Figure 11. Amount of force between the tool and the sample.

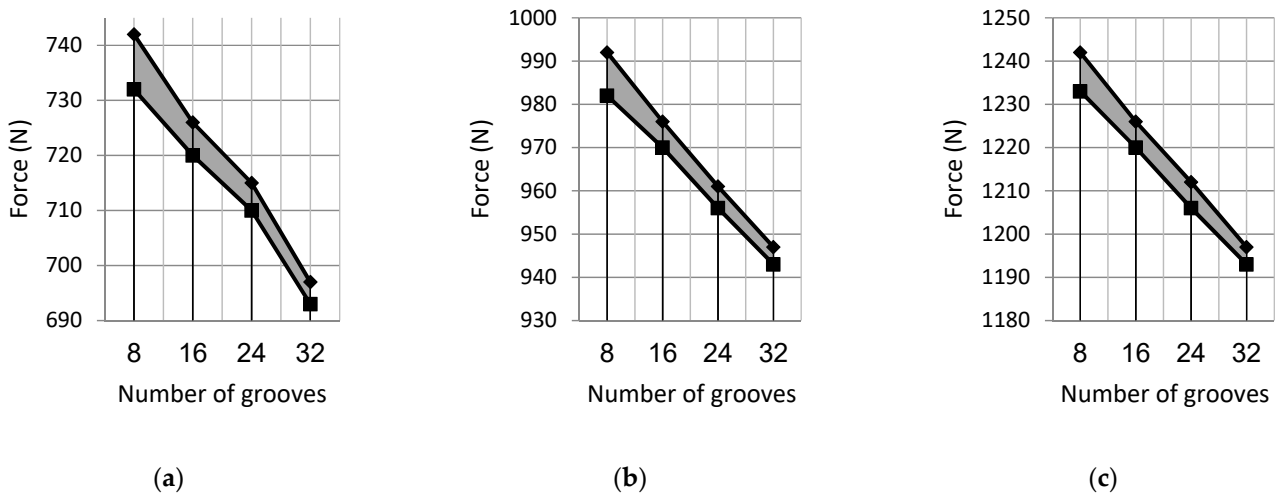


Figure 12. The amplitude of the force of the tool with a groove width of 4 mm on the part in the contact zone: (a) pressure of 750 N; (b) pressure of 1000 N; (c) pressure of 1250 N (■—minimum value of force; ◆—maximum value of force).

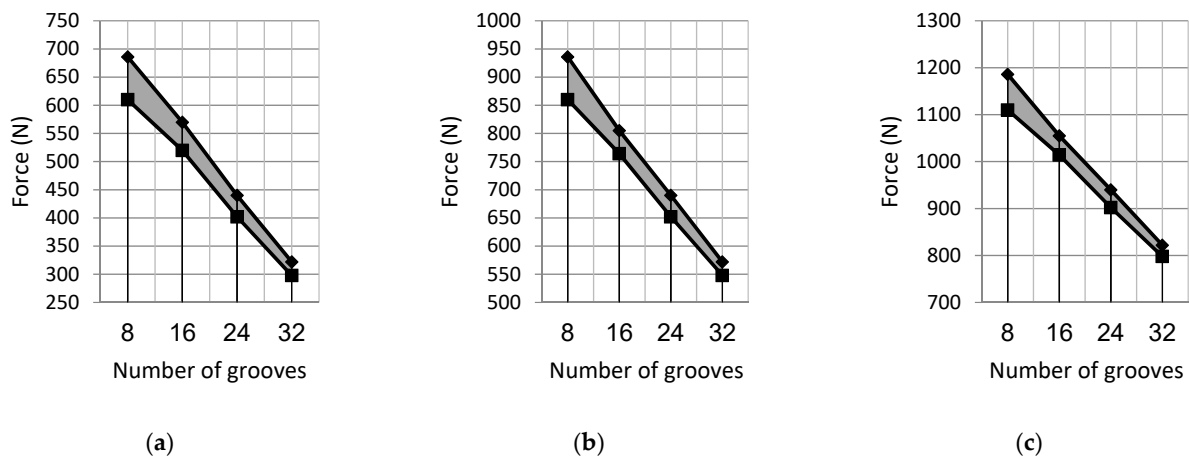


Figure 13. The amplitude of the force of the tool with a groove width of 8 mm on the part in the contact zone: (a) pressure of 750 N, (b) pressure of 1000 N, and (c) pressure of 1250 N (■—minimum value of force; ◆—maximum value of force).

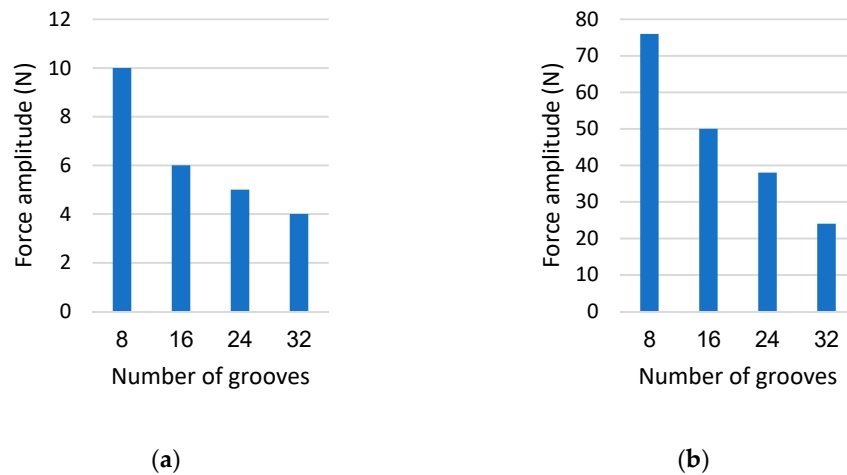


Figure 14. Force amplitude of the reaction of the tool to the part: (a) groove width: 4 mm; (b) groove width: 8 mm.

An important factor for the formation of nanocrystal layers is the frequency of impact of the tool with the part. It has been shown that as the number of grooves increases, the frequency of impacts in the treatment area increases significantly. Thus, when the number of grooves is equal to eight, the frequency of impact of the tool on the part is equal to 750 Hz, and when the quantity of grooves is equal to 32, the frequency of impact of the tool on the part is equal to 2.5 kHz (Figure 15).

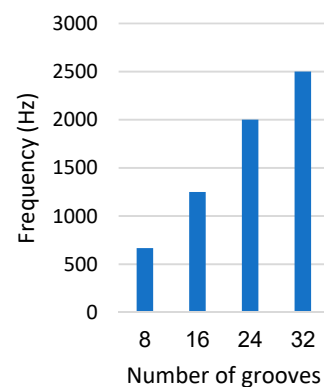


Figure 15. The frequency of the mutual displacement of the part and the tool in the area of their contact.

Experimental studies have shown that during thermo-deformation strengthening of flat surfaces of samples made of steel 41Cr4, the tangential and normal components of the friction force in the tool–sample contact zone have a wave-like character (Figure 16). The amplitude of the change in the components of the friction force is 0.15–0.25 of the magnitude of the force. The highest value is reached by the normal component of the friction force in the tool–part contact zone. The processing modes significantly affect the value, especially the amount of vertical tension. It determines the amount of pressing of the tool to the processed surface of the part. The nature of the change in the tangential component of the force, which occurs in the contact zone of the tool with the processed surface of the samples, is similar to that of the normal component and corresponds to the change in the geometry of the working surface of the tool. The amount of loading and unloading of a unit area of contact of the tool with the processed surface depends on the processing modes (linear speed on the periphery of the tool and speed of movement of the machine table) and the number of grooves. Accordingly, the movement of the tool along the processed surface is interrupted. Due to the specified processes, we obtained a wave-like character of changes in the components of the friction force during thermo-deformation strengthening.

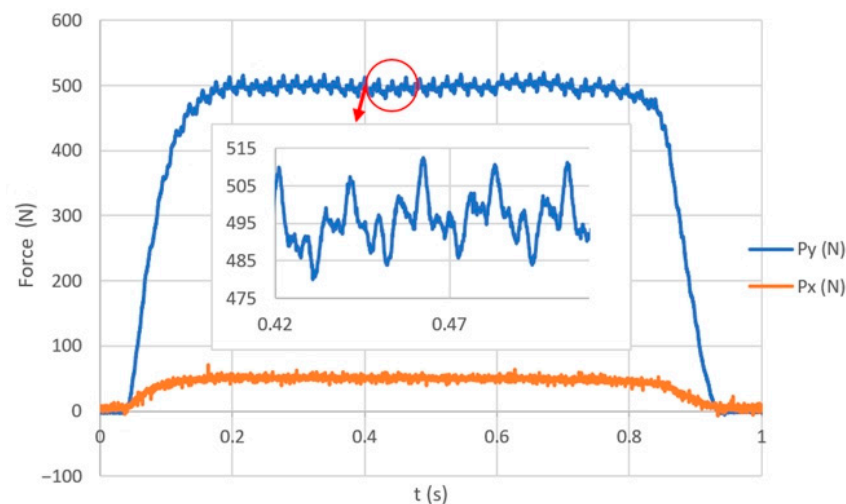


Figure 16. Normal (P_y) and tangential (P_x) components of the forces that occur during the strengthening of flat surfaces.

The formation of strengthened layers with a nanocrystalline structure is intensified by increasing the intensity of deformation of the contact zone on the treated surface by a tool with transverse grooves on its periphery. The metal of the surface layer is cyclically loaded and unloaded, as well as heated and cooled, during the alternate passage of the smooth surface and the groove along the surface of the tool's contact zone with the sample. The contact zone of the tool with the processed surface during thermo-deformation strengthening is heated to temperatures close to the melting point [24]. At such high temperatures, the metal softens, and its plasticity increases. After the groove passes over the contact zone, the next smooth surface comes into contact and creates a shock load on the contact zone. Such processes intensify the deformation of the surface layer of the metal to a greater depth, contribute to grain grinding, and form a strengthened layer to a greater depth.

The thickness of the strengthened layer and its hardness obtained during thermo-deformation strengthening of flat samples made from steel 41Cr4 (quench-hardening and low-temperature tempering) significantly affect the shape of the working surface of the tool, as shown by conducted metallographic studies. Thus, during thermo-deformation strengthening with a tool with a smooth working surface, the thickness of the hardened layer was 140–160 microns, and the hardness was 8.6 GPa (with a hardness of the base metal of 5.6 GPa) (Figure 17). During thermo-deformation strengthening with a tool with transverse grooves on its working part, the thickness of the hardened layer and its hardness

increase. When processing with a tool with 24 transverse grooves with a width of 3–4 mm, the thickness of the layer increased to 190–220 μm , and the hardness increased to 9.3 GPa. When the width of the transverse grooves increased to 8–9 mm, the thickness of the layer increased to 250–260 μm , and the hardness increased to 11.1 GPa. A further increase in the width of the grooves led to a certain decrease in the thickness of the strengthened layer. The use of a tool with transverse grooves leads to an intensification of the plastic deformation of the surface layer of the metal during thermo-deformation strengthening, which also leads to a decrease in grain size, which increases by about 10 nm near the surface. The grain size of the strengthened layers obtained by strengthening with a tool with a smooth part is much larger and is 60–80 nm. The resulting strengthened layers are nanocrystalline. The metallographic structure of steel 41Cr4 is shown in Figure 18.

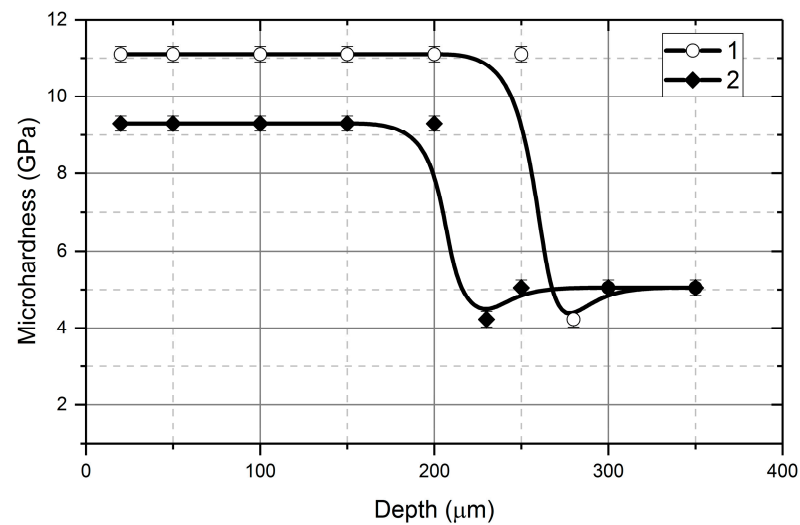


Figure 17. Microhardness of steel after thermo-deformation treatment 41Cr4: 1—length of grooves: 4 mm; 2—length of grooves: 8 mm.

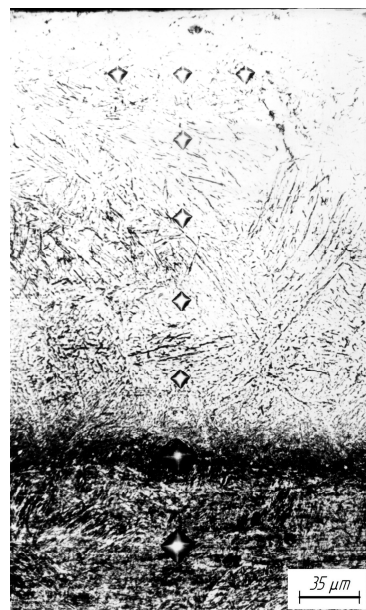


Figure 18. Structure of steel 41Cr4 after thermo-deformation treatment (length of grooves: 8 mm).

The conducted experimental studies confirm our theoretical calculations.

4. Conclusions

Thermo-deformation strengthening of the surface layers of parts using a tool with transverse grooves on its working peripheral surface combines two methods of forming a strengthened layer with a nanocrystalline structure—the action of a high-intensity heat source and intense plastic deformation.

Intensive plastic deformation of the metal of the surface layer of the sample is achieved by alternately passing the smooth tool surface and the groove through the contact zone of the tool and the sample, during which time the contact zone is cyclically loaded and unloaded.

The design scheme of the elastic system of a surface grinding machine was developed to study the dynamic processes that take place during thermo-deformation strengthening of flat surfaces of samples in the contact zone between the tool and the treated surface.

When the width of the groove increases, the difference between the maximum and minimum amount of the amplitude of the reaction force, which occurs in the contact zone between the tool and the processed surface, increases. Thus, when using a tool with eight grooves with a width of 4 mm on its working surface (pressing force 750 N), the difference between the amounts of the force amplitude was equal to 10 N. When the groove width was 8 mm, the difference in the force amplitude increased by 7.5 times and was 75 N. With an increase in the force of pressing the tool to the processed surface with the same width of the groove, it did not affect the magnitude of the change in the amplitude of the force in the contact zone.

Experimental studies have shown that during the thermal deformation treatment (strengthening) of samples made of steel 41Cr4, the thickness and microhardness of the strengthened layer increase with the increase in the groove width on the working part of the tool. For example, with a groove width of 3–4 mm, the thickness of the strengthened layer was 190–220 μm , and its microhardness was 9.3 GPa. With an increase in the groove width of 9 mm, the thickness and microhardness of the layer increased to 250–260 μm and 11.1 GPa, respectively.

Author Contributions: Conceptualization, V.G., I.H. and T.H.; methodology, I.H., V.G. and P.M.; validation, I.H., P.M. and T.H.; formal analysis, V.G., P.M., I.H., V.D., T.H. and W.W.; investigation, I.H., V.G. and W.W.; writing—original draft preparation, V.G., P.M., I.H., V.D., T.H. and W.W.; writing—review and editing, I.H., P.M. and V.G.; visualization, V.G. and V.D.; supervision, I.H. and P.M. All authors have read and agreed to the published version of the manuscript.

Funding: This research received no external funding.

Data Availability Statement: The data presented in this study are available on request from the corresponding author.

Conflicts of Interest: The authors declare no conflict of interest.

References

1. Davis, J.R. *Surface Engineering for Corrosion and Wear Resistance*; ASM International: Geauga County, OH, USA, 2001; ISBN 0-87170-700-4.
2. Dwivedi, D.K. *Surface Engineering: Enhancing Life of Tribological Components*; Springer: New Delhi, India, 2018; ISBN 978-81-322-3777-8.
3. Troshchenko, V.T. *Deformation and Destruction of Metals under Multicycle Loading*; Naukova Dumka: Kyiv, Ukraine, 1981.
4. Pineau, A.; McDowell, D.L.; Busso, E.P.; Antolovich, S.D. Failure of Metals II: Fatigue. *Acta Mater.* **2016**, *107*, 484–507. [[CrossRef](#)]
5. Santecchia, E.; Hamouda, A.M.S.; Musharavati, F.; Zalnezhad, E.; Cabibbo, M.; El Mehtedi, M.; Spigarelli, S. A Review on Fatigue Life Prediction Methods for Metals. *Adv. Mater. Sci. Eng.* **2016**, *2016*, 9573524. [[CrossRef](#)]
6. Melters, P.M. *Introduction to Metal Fatigue*; Aarhus University: Aarhus, Denmark, 2018; ISBN 2245-4594.
7. Troshchenko, V.T.; Khamaza, L.A. Stages of Fatigue Failure of Metals and Alloys. *Rep. Natl. Acad. Sci. Ukr.* **2018**, *2*, 56–63. [[CrossRef](#)]
8. Yushchenko, K.A.; Borysov, Y.S.; Kuznetsov, V.D.; Korzh, V.M. *Surface Engineering*; Naukova Dumka: Kyiv, Ukraine, 2007.
9. Gurey, V.; Hurey, I. The Effect of the Hardened Nanocrystalline Surface Layer on Durability of Guideways. In *Proceedings of the Lecture Notes in Mechanical Engineering*; Tonkonogyi, V., Ivanov, V., Trojanowska, J., Oborskyi, G., Edl, M., Kuric, I., Pavlenko, I., Dasic, P., Eds.; Springer International Publishing: Cham, Switzerland, 2020; pp. 63–72.

10. Gurey, V.; Hurey, I.; Hurey, T.; Wojtowicz, W. Fatigue Strength of Steel Samples After Friction Treatment. *Lect. Notes Mech. Eng.* **2023**, *1*, 274–283. [[CrossRef](#)]
11. Kyryliv, V.I.; Gurey, V.I.; Maksymiv, O.V.; Hurey, I.V.; Kulyk, Y.O. Influence of the Deformation Mode on the Force Conditions of Formation of the Surface Nanostructure of 40Kh Steel. *Mater. Sci.* **2021**, *57*, 422–427. [[CrossRef](#)]
12. Shaw, L.L. The Surface Deformation and Mechanical Behavior of Nanostructured Alloys. In *Nanostructured Metals and Alloys*; Elsevier: Cambridge, UK, 2011; pp. 481–506, ISBN 9781845696702.
13. Bartkowska, A. Production and Properties of FeB-Fe₂B-Fe₃(B,C) Surface Layers Formed on Tool Steel Using Combination of Diffusion and Laser Processing. *Coatings* **2020**, *10*, 1130. [[CrossRef](#)]
14. Korzhyk, V.; Tyurin, Y.; Kolisnichenko, O. *Theory and Practice of Plasma-Detonation Technology of Surface Hardening Metal Products*; Privat Company Technology Center: Kharkiv, Ukraine, 2021; ISBN 9786177319466.
15. Lukaszewicz, K. Review of Nanocomposite Thin Films and Coatings Deposited by PVD and CVD Technology. In *Nanomaterials*; Rahman, M.M., Ed.; InTech: Rijeka, Croatia, 2011.
16. Quintino, L. Overview of Coating Technologies. In *Surface Modification by Solid State Processing*; Elsevier: Cambridge, UK, 2014; pp. 1–24, ISBN 9780857094681.
17. Hurey, I.; Hurey, T.; Lanets, O.; Dmyterko, P. The Durability of the Nanocrystalline Hardened Layer during the Fretting Wear. *Lect. Notes Mech. Eng.* **2021**, *2*, 23–32. [[CrossRef](#)]
18. Vilaça, P. Friction Surfacing. In *Surface Modification by Solid State Processing*; Elsevier: Cambridge, UK, 2014; pp. 25–72.
19. Zhang, F.; Duan, C.; Wang, M.; Sun, W. White and Dark Layer Formation Mechanism in Hard Cutting of AISI52100 Steel. *J. Manuf. Process.* **2018**, *32*, 878–887. [[CrossRef](#)]
20. Zhang, F.; Duan, C.; Sun, W.; Ju, K. Effects of Cutting Conditions on the Microstructure and Residual Stress of White and Dark Layers in Cutting Hardened Steel. *J. Mater. Process. Technol.* **2019**, *266*, 599–611. [[CrossRef](#)]
21. Javaheri, V.; Sadeghpour, S.; Karjalainen, P.; Lindroos, M.; Haiko, O.; Sarmadi, N.; Pallaspuuro, S.; Valtonen, K.; Pahlevani, F.; Laukkanen, A.; et al. Formation of Nanostructured Surface Layer, the White Layer, through Solid Particles Impingement during Slurry Erosion in a Martensitic Medium-Carbon Steel. *Wear* **2022**, 496–497, 204301. [[CrossRef](#)]
22. Inoue, A.; Hashimoto, K. (Eds.) *Amorphous and Nanocrystalline Materials*; Advances in Materials Research; Springer: Berlin/Heidelberg, Germany, 2001; Volume 3, ISBN 978-3-642-08664-9.
23. Hosseini, S.B.; Klement, U. A Descriptive Phenomenological Model for White Layer Formation in Hard Turning of AISI 52100 Bearing Steel. *CIRP J. Manuf. Sci. Technol.* **2021**, *32*, 299–310. [[CrossRef](#)]
24. Gurey, V.; Shynkarenko, H.; Kuzio, I. Mathematical Model of the Thermoelasticity of the Surface Layer of Parts during Discontinuous Friction Treatment. *Lect. Notes Mech. Eng.* **2021**, *2*, 12–22. [[CrossRef](#)]
25. Wu, S.; Liu, G.; Zhang, W.; Chen, W.; Wang, C. Formation Mechanism of White Layer in the High-Speed Cutting of Hardened Steel under Cryogenic Liquid Nitrogen Cooling. *J. Mater. Process. Technol.* **2022**, *302*, 117469. [[CrossRef](#)]
26. Lowe, T.C.; Zhu, Y.T.; Semiatin, S.L.; Berg, D.R. Overview and Outlook for Materials Processed by Severe Plastic Deformation. In *Investigations and Applications of Severe Plastic Deformation*; Lowe, T.C., Valiev, R.Z., Eds.; Springer: Dordrecht, The Netherlands, 2000; pp. 347–356, ISBN 978-94-011-4062-1.
27. Hahn, H. Unique Features and Properties of Nanostructured Materials. In *Nanomaterials by Severe Plastic Deformation*; Wiley-VCH Verlag GmbH & Co., KGaA: Weinheim, Germany, 2005; pp. 2–17, ISBN 9783527602469.
28. Guo, Y.B.; Warren, A.W.; Hashimoto, F. The Basic Relationships between Residual Stress, White Layer, and Fatigue Life of Hard Turned and Ground Surfaces in Rolling Contact. *CIRP J. Manuf. Sci. Technol.* **2010**, *2*, 129–134. [[CrossRef](#)]
29. Cicero, S.; Álvarez, J.A. Fracture, Fatigue, and Structural Integrity of Metallic Materials. *Metals* **2019**, *9*, 913. [[CrossRef](#)]
30. Kyryliv, V.; Maksymiv, O.; Gurey, V.; Hurey, I.; Kyryliv, Y.; Zvirko, O. The Mode Deformation Effect on Surface Nanocrystalline Structure Formation and Wear Resistance of Steel 41Cr4. *Coatings* **2023**, *13*, 249. [[CrossRef](#)]
31. Hurey, I.; Gurey, V.; Kyryliv, V. A Tool for Alloying the Surface Layers of Machine Parts. Patent No. 123883, 2021.
32. Burek, J.; Hurey, I. Tool for Forming a Nanocrystalline Hardened Surface Layer of an Object and a Method for Forming a Nanocrystalline Hardened Surface Layer of an Object. Patent No. 240972, 2022.
33. Gans, R.F. *Engineering Dynamics*; Springer: New York, NY, USA, 2013; ISBN 978-1-4614-3929-5.
34. Timoshenko, S.; Weaver, W. *Vibration Problems in Engineering*; Wolfenden Press: Singapore, 2007; ISBN 978-1406774658.
35. Torby, B.J. *Advanced Dynamics for Engineers*; Holt Rinehart & Winston: New York, NY, USA, 1984; ISBN 0-03-063366-4.
36. Goldstein, H.; Poole, C.; Safko, J. *Classical Mechanics*, 3rd ed.; Addison Wesley: Boston, MA, USA, 2001; ISBN 9780201657029.
37. Taylor, R.J. *Classical Mechanics*; University Science Books: Melville, NY, USA, 2005; ISBN 1-891389-22-X.

Disclaimer/Publisher’s Note: The statements, opinions and data contained in all publications are solely those of the individual author(s) and contributor(s) and not of MDPI and/or the editor(s). MDPI and/or the editor(s) disclaim responsibility for any injury to people or property resulting from any ideas, methods, instructions or products referred to in the content.